Infrared Spectrum of the $Ar-NH_2^+$ Ionic Complex

O. Dopfer,* S. A. Nizkorodov, R. V. Olkhov, and J. P. Maier

Institut für Physikalische Chemie, Universität Basel, Klingelbergstrasse 80, CH-4056 Basel, Switzerland

K. Harada

Department of Chemistry, Faculty of Science, Kyushu University 33, Hakozaki, Higashi-ku, Fukuoka 812-81, Japan

Received: July 23, 1998; In Final Form: September 22, 1998

Rotationally resolved infrared spectra of the ν_1 and ν_3 N−H stretching vibrations of the $Ar-NH_2^+$ radical ionic complex have been observed by means of photodissociation spectroscopy. The analysis of the rotational structure shows that the complex has a $^3\Sigma^-$ ground electronic state with a linear or quasi-linear proton-bound structure $Ar-H-N-H^+$ characterized by an intermolecular center of mass separation of 3.085 Å. The origins of the ν_1 and ν_3 bands were determined as 2803.65(2) and 3287.36(2) cm^{-1}, and the frequency of the intermolecular stretch vibration, ν_s, as 170.4(6) cm^{-1}. Ab initio calculations performed at the UMP2 level of theory confirm that the quasi-linearity and the diradical character of NH_2^+ in its electronic ground state are not changed upon Ar complexation. The calculated properties of the intermolecular bond of the complex (D_e = 1773 cm^{-1}, $R_{Ar-H} \sim 2.01$ Å, $\nu_s \sim 185$ cm^{-1}) and the predicted complexation induced frequency shifts for ν_1 and ν_3 are in good agreement with the experimental results.

1. Introduction

It is well-established that intermolecular forces play an important role in many areas of physics, chemistry, and biology.[1,2] To understand these interactions from the microscopic point of view, detailed knowledge of the intermolecular potential describing the interaction between the considered species is required. In the last two decades, through the application of high-resolution spectroscopic techniques, substantial progress has been achieved in the characterization of intermolecular interaction potentials acting in neutral complexes.[3−7] Owing to fruitful interplay between experiment and theory, accurate intermolecular potential energy surfaces of a few small dimers and trimers are now available.[8−11]

In contrast to neutral clusters, for ionic complexes high-resolution spectroscopic data are fewer,[12−16] mainly owing to the experimental difficulties involved in the production of sufficient number densities. The interest in charged species arises partly from the fact that, owing to the electrostatic and induction interactions caused by the additional charge, the bond strengths and bond lengths in ionic complexes are intermediate between strong chemical and weak neutral van der Waals bonds. The usually small concentration of cluster ions in practically all used ion sources requires highly sensitive spectroscopic techniques. Though recently a few complexes have been studied by direct absorption techniques,[17−20] most high-resolution spectra obtained so far have been recorded by photodissociation of mass-selected species,[12,21] and it is by this approach that the infrared (IR) spectrum of $Ar-NH_2^+$ has been recorded.

The $Ar-NH_2^+$ complex is a further member in a series of proton-bound complexes of the type $B-HA^+$ that have been characterized by their IR photodissociation spectra in our laboratory. Thermochemical studies show that the stability of such complexes is related to the difference in the proton affinities (PA) of the two bases A and B.[22] As for all of the complexes studied so far the proton affinity of the base A (CO, N_2, SiO, NH_3, O_2, O) exceeded by far the one of B (B = He, Ne, Ar, H_2), they can be considered as HA^+ ions weakly distorted by the ligand B.[23−30] The degree of proton transfer from base A to base B is correlated to the strength of the intermolecular bond and the accompanying destabilization of the intramolecular H−A bond. For example, for the $Rg-HCO^+$ series (Rg = He, Ne, Ar) a linear dependence between the complexation-induced red shift of the C−H stretch frequency and the PA of the Rg atom has been found.[31]

The $Ar-NH_2^+$ complex has been chosen for several reasons. (1) Neither spectroscopic nor theoretical data are available for complexes composed of NH_2^+ and neutral ligands. (2) NH_2^+ is quasi-linear in its electronic ground state with a very low barrier to linearity, so that even complexation with an inert ligand like Ar might significantly change the potential along the intramolecular bending coordinate. The IR spectrum of the complex will be characteristic of either a bent or a linear molecule depending on whether Ar complexation does or does not lead to a significant increase of the barrier. (3) NH_2^+ is a diradical in its electronic ground state. Only recently has an advanced theoretical treatment of floppy molecular complexes containing diradicals been developed,[32,33] and there has been a lack of high-resolution spectroscopic data on such complexes, the two notable exceptions being the neutral O_2-N_2O complex[34] and the cationic OH^+−He/Ne clusters.[30] As the parameter describing the spin−spin interaction in diradical complexes contains valuable information on the angular anisotropy of the potential, the spectra of complexes of NH_2^+ (which is isoelectronic to OH^+) with rare gas atoms provide information about the magnitude of the angular rigidity in such open shell ionic complexes.

The NH_2^+ ion, serving as the mid-infrared chromophore in the $Ar-NH_2^+$ complex, is of importance in interstellar chemistry of nitrogen-bearing molecules[35−38] and plasmas containing

10.1021/jp983132b CCC: $15.00
Published on Web 11/14/1998

molecular hydrogen and nitrogen. It is isoelectronic to CH_2, and the properties of its low-lying electronic states have been investigated by numerous ab initio calculations.[39−47] The structure in the $^3B_1$ ground state is bent ($\theta \sim 153°$, $r_{N-H} \sim 1.029$ Å); however, the barrier to linearity ($V_b \sim 200$ cm^{-1}) lies below the zero-point level of the bending vibration. Therefore, NH_2^+ can be considered as a quasi-linear molecule with a $^3\Sigma_g^-$ ground state (in $D_{\infty h}$). The correlation between the rovibrational quantum numbers of the bent and the linear configuration of triatomic molecules has been outlined in ref 45. Rovibrational calculations on the most recent ab initio surface gave the following frequencies for the three fundamentals:[46] $\nu_1 = 3136$ cm^{-1} (symmetric N−H stretch), $\nu_3 = 3384$ cm^{-1} (asymmetric N−H stretch), $\nu_2^{bent} = 943$ cm^{-1}, and $\nu_2^{linear} = 336$ cm^{-1} (H−N−H bend).

In contrast to the theoretical side, less experimental spectroscopic information is available for the ground state of NH_2^+. The ν_2 frequency was derived as 940 ± 50 cm^{-1} from a photoelectron spectrum of NH_2,[48] and the separation to the first excited state ($^1A_1$) was measured as 1.305 ± 0.01 eV via photoionization efficiency measurements.[49] High-resolution infrared absorption spectra of the ν_3 (at 3359.9 cm^{-1}) and associated sequence bands yielded molecular constants for the vibrational ground state, all three fundamentals, and several overtones and combination bands.[50,51]

Complexation of the NH_2^+ ion with Ar has several effects on its properties. (1) Both the ab initio calculations and the experimental data presented below indicate that the Ar ligand is linearly bound to one of the protons, with little effect on the barrier to quasi-linearity of the monomer. Thus, the complex can also be treated as a (quasi-)linear species, and throughout this paper the linear molecule notation will be used for the analysis of the experimental data. (2) In the complex ($C_{\infty v}$) the inversion symmetry of the quasi-linear monomer ($D_{\infty h}$) is lifted, and the rovibrational selection rules and the nuclear spin statistical weights change as well. (3) The proton involved in the intermolecular bond ("bound H") is slightly transferred from N to Ar resulting in a destabilization of this N−H bond upon complexation. This effect, together with the modification of the normal coordinates, can be monitored by following the complexation-induced frequency shifts of the N−H stretch vibrations.

2. Experimental Section

Infrared spectra of the Ar−NH_2^+ complex have been obtained by means of photodissociation spectroscopy in a tandem mass spectrometer. The experimental setup has been described in detail previously.[52,53] The parent complex was produced in an electron impact ion source by expanding a mixture of Ar, He, and NH_3 in a ratio of approximately 15:1:0.001 at a backing pressure of 3 bar through a pulsed nozzle. The first quadrupole mass spectrometer selected Ar−NH_2^+ out of the variety of ions present in the skimmed supersonic expansion. Subsequently, the parent ion beam was injected through a 90° quadrupole deflector into an octopole ion guide where it was overlapped in space and time with a counterpropagating infrared laser pulse (bandwidth 0.02 cm^{-1}) emitted by an optical parametric oscillator (OPO) laser system. The absorbed photon energy exceeded the lowest dissociation limit of the cluster ion and eventually induced its fragmentation into NH_2^+ and Ar. The produced fragment ions were filtered by the second quadrupole mass spectrometer and finally sensed with a Daly detector.[54] Photofragmentation spectra of Ar−NH_2^+ were recorded by monitoring the NH_2^+ fragment current as a function of the IR laser frequency. To compensate for any background signal, mainly caused by metastable decomposition of hot parent species in the octopole, the ion source was triggered at twice the laser frequency (20 Hz), and the signal with the laser off was subtracted from that with the laser on. The fragment ion signal was normalized for laser pulse intensity variations measured with an InSb IR detector.

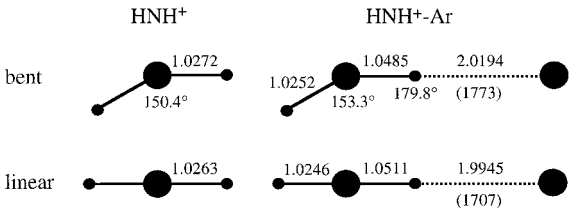

Figure 1. Calculated structures of the bent (global minima) and linear (transition states) configurations of NH_2^+ and Ar−NH_2^+. Distances are given in Å, and the binding energies (D_e) of the intermolecular bonds (in brackets) are given in cm^{-1}.

The laser frequency was calibrated by Etalon fringes of the OPO and simultaneously recorded optoacoustic spectra of HDO, C_2H_2, and NH_3 utilizing the signal and idler outputs of the OPO.[55] The transition frequencies have been corrected for the Doppler shift caused by the 5 ± 1 eV kinetic energy of the parent ions in the octopole. The absolute precision of the calibration is limited to 0.01 cm^{-1} by a combination of the OPO bandwidth and the uncertainty in the kinetic energy of the ions.

3. Ab Initio Calculations

The experimental approach is complemented by ab initio calculations employing the GAUSSIAN 94 program package.[56] The aim of these calculations was to estimate the effects of Ar complexation on the properties of the NH_2^+ monomer (e.g., geometry, vibrational frequencies, and barrier to linearity) as well as to characterize features of the intermolecular interaction in the complex (e.g., intermolecular separation, binding energy, and intermolecular frequencies).

The electronic ground states of the NH_2^+ monomer and Ar−NH_2^+ dimer have been investigated at the UMP2 level of theory. The basis set contained Ahlrichs VTZ functions for the core electrons, which were augmented with diffuse and polarization functions taken from the aug-cc-pVTZ basis set.[57] The contraction scheme can be described as N(11s, 7p, 3d, 2f) → (7s, 4p, 3d, 2f), H(6s, 3p, 2d) → (4s, 3p, 2d), and Ar(13s, 10p, 3d, 2f) → (8s, 6p, 3d, 2f). All coordinates were allowed to relax during the search for stationary points. Calculated binding energies of the dimer were corrected for the basis set superposition error[58] and the relaxation energy arising from the deformation of NH_2^+ upon complex formation.[59] The results of the calculations are summarized in Figure 1 and Table 1. Harmonic vibrational frequencies were scaled by a factor of 0.940 12 to match the experimental ν_3 frequency of NH_2^+ with that calculated for the linear configuration. The linear geometry was preferred to the bent one for the determination of the scaling factor, as the quasi-linearity of NH_2^+ is maintained in the Ar−NH_2^+ dimer.

Geometry optimizations at the employed level of theory led to a bent equilibrium structure for NH_2^+, with a bond angle (150.4°) and an N−H separation (1.027 Å) in close agreement with previous calculations. The linear transition state lies 152 cm^{-1} higher in energy and features a slightly shorter N−H bond (1.026 Å) compared to the bent geometry. As expected, neither of the ν_1 or ν_3 frequencies depend strongly on the bending angle. For quasi-linear triatomic molecules the harmonic approach

TABLE 1: Geometries (in Å) and Scaled Harmonic Frequencies (in cm^{-1}) of the Bent and Linear Configurations of NH_2^+ and $Ar-NH_2^+$ (Ar−H1−N−H2) Obtained from the UMP2 Calculations (See Figure 1)[a]

species (symmetry)	$r_{N-H1/2}$ (r_{N-H1}/r_{N-H2})	R_{Ar-H1}	∠H1−N−H2	∠Ar−H1−N
NH_2^+ (C_{2v})	1.0272		150.4°	
NH_2^+ ($D_{\infty h}$)	1.0263		180.0°	
$Ar-NH_2^+$ (C_s)	1.0485/1.0252	2.0194	153.3°	179.8°
$Ar-NH_2^+$ ($C_{\infty v}$)	1.0511/1.0246	1.9945	180.0°	180.0°

species (symmetry)	ν_3	ν_1	ν_2	ν_s	ν_b
NH_2^+ (C_{2v})	3339.5 (637/b_2)	3088.0 (37/a_1)	770.6 (143/a_1)		
NH_2^+ ($D_{\infty h}$)	3359.9 (807/σ_u^+)	3070.1 (0/σ_g^+)	571.0*i* (389/π_u)		
$Ar-NH_2^+$ (C_s)	3270.4 (740/a′)	2814.1 (1045/a′)	777.6 (94/a′)	178.9 (91/a′)	274.4 (16/a′) 462.0 (55/a″)
$Ar-NH_2^+$ ($C_{\infty v}$)	3278.6 (868/σ_g)	2761.6 (1181/σ_g)	222.7*i* (62/π)	187.8 (96/σ_g)	455.3 (220/π)

[a] IR intensities (in km/mol) and vibrational symmetries are given in brackets.

usually fails to predict reliable experimental bending frequencies. Therefore, the ν_2 frequencies in Table 1 cannot directly be related to experimental data, and they are only listed for completeness.

The most stable structure of the $Ar-NH_2^+$ dimer corresponds to a proton-bound configuration where the Ar ligand forms an almost linear Ar−H−N bond to the bent NH_2^+ ion. The intermolecular bond is characterized by a well depth $D_e = 1773$ cm^{-1}, an Ar−H separation of $R_{Ar-H} = 2.02$ Å, and an intermolecular stretching frequency $\nu_s = 179$ cm^{-1}. A significant transfer of the bound proton (H1 in Table 1) toward the Ar atom is evident from the lengthening of the respective N−H bond by 0.02 Å. On the other hand, the free N−H bond is almost unaffected. The barrier to quasi-linearity is reduced to 66 cm^{-1} upon complexation and, apart from the H−N−H angle, the structure and energetics of the linear transition state are similar to those of the bent global minimum. This concerns in particular the intermolecular bond (e.g., D_e, ν_s, and R_{Ar-H}) as well as the complexation-induced frequency shifts of the N−H stretching vibrations (ν_1 and ν_3).

Complexation with Ar has a drastic influence on the direction of the normal coordinates of the N−H stretch vibrations. The symmetric (ν_1) and antisymmetric (ν_3) N−H stretch modes of the monomer transform to vibrations in the complex that can be characterized to a good approximation by a bound and free N−H stretch, respectively. This results in a large complexation-induced red shift of 274 (309) cm^{-1} for ν_1, and a somewhat smaller one of 69 (81) cm^{-1} for ν_3 in the bent (linear) configuration. Owing to the inversion symmetry, the ν_1 vibration is IR-forbidden in the monomer. However, as complexation breaks this symmetry, the ν_1 mode becomes infrared-allowed in $Ar-NH_2^+$, and according to the calculation its oscillator strength even exceeds that of the strong IR active ν_3 mode.

The binding energy of the C_{2v} structure with the Ar atom bound to the N atom ($R_{Ar-N} = 2.725$ Å) was calculated as 967 cm^{-1}. The derived barrier for the internal rotation of NH_2^+ within the complex, $V_b = 806$ cm^{-1}, is sufficiently high to completely quench the effects of this internal motion at the spectral resolution available in the present experiment.

4. Spectrum and Vibrational Assignment

Figure 2 reproduces an overview of the recorded photodissociation spectrum of $Ar-NH_2^+$ in the range of 2500−3600 cm^{-1}. As the spectrum is composed of several shorter scans that were recorded separately, only the relative intensities of closely spaced transitions are reliable. The spectrum is dominated by two strong transitions centered at 2804 and 3287 cm^{-1}, and their Σ−Σ type rotational substructure confirms the quasi-linear geometry of the complex. By comparison with the ab initio calculations, they can be safely attributed to the ν_1 and ν_3 fundamentals of the complex. The predicted frequencies of around 2790 and 3275 cm^{-1} (averages of the values calculated for the linear and bent geometries) agree well with the experimental values. Moreover, the intensity of the ν_1 band, which is zero for the monomer, exceeds that of the strong ν_3 transition of the complex, consistent with the calculated IR intensities (Table 1).

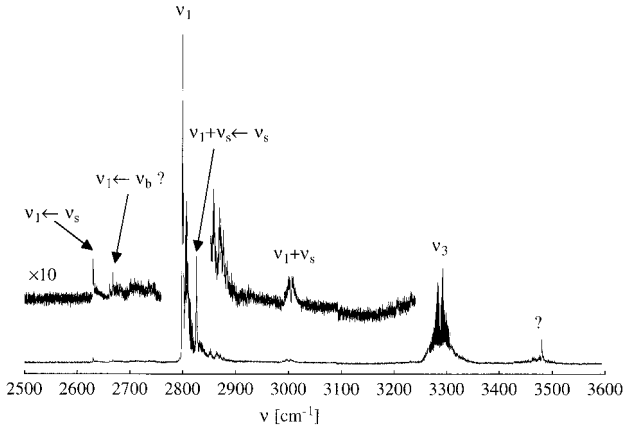

Figure 2. Overview of the observed photodissociation spectrum of $Ar-NH_2^+$. Selected parts of the spectrum are vertically expanded by a factor of 10 to show the weak features. As the whole spectrum is composed of several scans, the relative intensities of widely spaced transitions are only approximate.

A weak Σ−Σ type band appears approximately 197 cm^{-1} to the blue of the ν_1 transition. Its position and strength suggest an assignment to the combination band $\nu_1 + \nu_s$, where ν_s denotes the intermolecular stretching vibration. Similar transitions have previously been observed for the related $Ar-HCO^+$ [52] and $He/Ne-HN_2^+$ [60,61] complexes.

Around 27 cm^{-1} above ν_1, a sequence band is observed that is attributed to $\nu_1 + \nu_s \leftarrow \nu_s$. From comparison with $\nu_1 + \nu_s$, the frequency of the intermolecular stretching frequency in the vibrational ground state can be inferred as 170 cm^{-1}, which

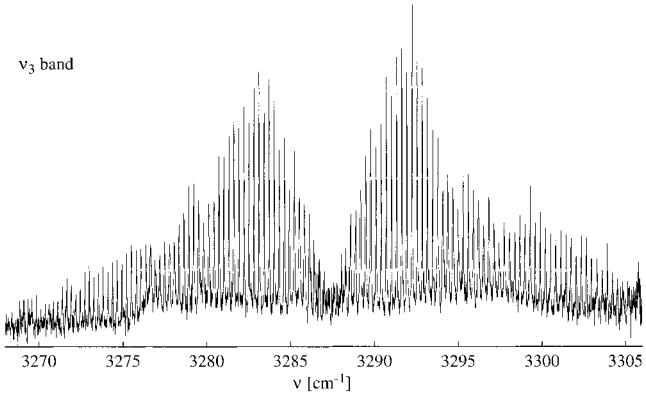

Figure 3. Photodissociation spectrum of the ν_3 band of $Ar-NH_2^+$.

corresponds closely to the calculated frequency of around 185 cm^{-1}. Moreover, the spectrum reveals a very weak $\Sigma-\Sigma$ type transition 170 cm^{-1} to the red of ν_1, which consequently can be interpreted as $\nu_1 \leftarrow \nu_s$ hot band. The analysis of the rotational substructure of the considered transitions supports these assignments (see below). Further sequence bands involving ν_1 are observed with rapidly decreasing intensity to the blue side of the ν_1 band, and they are almost certainly due to $\nu_1 + \nu_x \leftarrow \nu_x$, where ν_x are progressions and combinations of the intermolecular vibrations ($m\nu_s + n\nu_b$).

Near the $\nu_1 \leftarrow \nu_s$ hot band the spectrum shows another weak transition that contains a strong Q branch (2668 cm^{-1}) indicative of a $\Sigma-\Pi$ type band. Its position and strength is compatible with an assignment to the $\nu_1 \leftarrow \nu_b$ hot band, which would result in a frequency for the intermolecular bend (ν_b) of approximately 136 cm^{-1}. However, this interpretation is tentative. A further band with complicated structure is located near 3476 cm^{-1}, and its assignment is not obvious (see below).

5. Rotational Analysis

A (quasi-)linear structure of the complex has been assumed for the rotational analysis, because the spectrum did not show any evidence for a bent configuration of the $Ar-NH_2^+$ complex. As the splittings caused by the electron spin were resolved near the origin of the ν_3 band, a Hamiltonian was adopted that consisted of the usual terms for the rotational energy of a semirigid linear molecule including the electron spin interaction appropriate for a $^3\Sigma^-$ electronic state

$$H = BN^2 - DN^4 + {}^2/_3\lambda(3S_z^2 - S^2) + \gamma N\cdot S \qquad (1)$$

Here, B and D designate the rotational and centrifugal distortion constants while the third and fourth term correspond to the spin−spin and spin−rotation interaction, respectively. Hund's case (b) wave functions have been used to diagonolize the Hamiltonian matrix taken from Table 1a of ref 51, where the notation has been changed from α to $(2/3)\lambda$ and from $a - a_0$ to γ.

5.1. ν_3 Band. Figure 3 details the photodissociation spectrum obtained for the ν_3 band of $Ar-NH_2^+$, and Figure 4 shows an expanded view of this band near the band center. The fine structure caused by the electron spin interaction could be (at least partly) resolved for levels with J smaller than five. In total, more than 130 rotational lines could be assigned, with J quantum numbers ranging from 0 to 56. The observed lines are least-squares fitted to the transition frequencies calculated from the Hamiltonian in eq 1. In cases where the fine structure could not be resolved, the line was fitted to the estimated center of the rotational line derived from the Hamiltonian without the fine structure interaction.

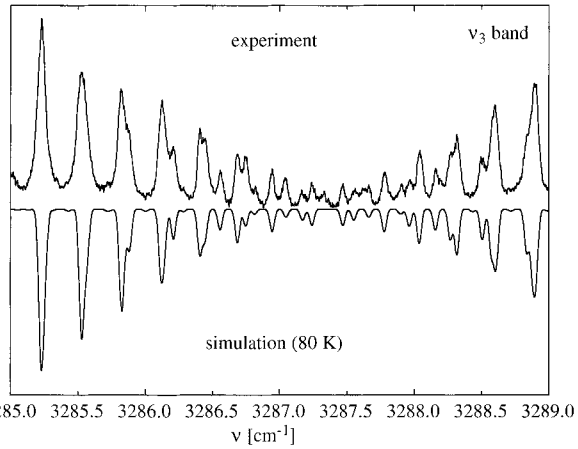

Figure 4. Central part of the experimental photodissociation spectrum of the ν_3 band of $Ar-NH_2^+$ (top) and a simulation utilizing the rotational constants of Table 2, a convolution width of 0.04 cm^{-1}, and a rotational temperature of 80 K.

TABLE 2: Molecular Constants (in cm^{-1}) of Various Vibrational States of $Ar-NH_2^+$[d]

constant	ν_3 band	ν_1 band
ν_0[a]	3287.356 99(81)	2803.647(11)
B'	0.152 040(25)	0.157 181(66)
D'	$4.467(59) \times 10^{-7}$	$3.68(59) \times 10^{-7}$
λ'	0.9020(61)	
γ'[b]	-2.24×10^{-4}	
B''	0.151 965(25)	0.151 965[c]
D''	$4.715(58) \times 10^{-7}$	4.715×10^{-7}[c]
λ''	0.9054(61)	
γ''[b]	-2.26×10^{-4}	

[a] Absolute accuracy of calibration is 0.01 cm^{-1}. [b] The spin−rotation constants were fixed to the estimated values derived from the spin−rotation constants of the monomer by scaling them with the ratio of the rotational constants. [c] Fixed to the values derived from the analysis of the ν_3 band. [d] Figures in parentheses are standard deviations. Experimental line positions are available from authors upon request.

The fits revealed weak perturbations for the upper state J levels between 24 and 30 and 35−39, which caused deviations from the unperturbed energies of up to 0.03 cm^{-1}. Since the perturbing states were not identified, these lines were excluded from the analysis. Finally, 103 weighted lines were fitted within 0.014 cm^{-1}, resulting in a standard deviation of 0.0054 cm^{-1}. These values are consistent with the observed line width of 0.04 cm^{-1}. A table listing the observed and calculated wavenumbers and the residuals of the fit is available upon request.

The molecular constants derived from the ν_3 band of the complex are listed in Table 2. The spin−spin interaction constant as well as the rotational and centrifugal distortion constants were determined for the ground and ν_3 states. Because the effects of the spin−rotation interaction were not prominent, the spin-rotation constants were fixed in both states to the values calculated from the corresponding spin−rotation constants of the NH_2^+ radical ion by scaling them with the ratio of the rotational constants of the complex and the monomer. Fixing these constants to zero affected the spin−spin interaction constants only within one standard deviation, whereas the effects on the other constants were negligible.

Figure 4 reproduces a simulation of the ν_3 band spectrum utilizing the molecular constants listed in Table 2, a convolution width of 0.04 cm^{-1}, and a rotational temperature of 80 K. Though this temperature was found to approximately reproduce the band envelope, the population of low J levels is better described by a lower temperature of 50 K while for the highest

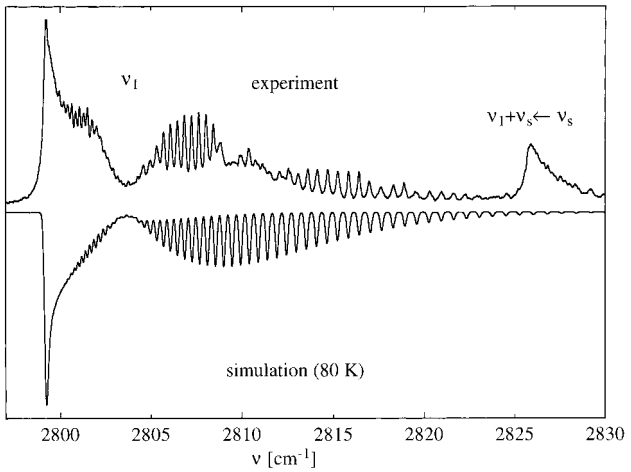

Figure 5. Experimental photodissociation spectrum of the ν_1 band of $Ar-NH_2^+$ (top) and a simulation utilizing the rotational constants of Table 2, a convolution width of 0.2 cm^{-1}, and a rotational temperature of 80 K. The formation of an early head in the P branch indicates the contraction of the intermolecular bond upon vibrational excitation.

observed J levels temperatures larger than 100 K are more appropriate. Similar nonthermal population distributions have previously been observed for other ionic complexes produced in the employed ion source.[24,30] The convolution width of 0.04 cm^{-1} is slightly larger than the laser resolution of 0.02 cm^{-1}. As the spectrum shown in Figure 4 was obtained by summing 20 single scans, calibration errors and averaging procedures might have slighly increased the observed bandwidth. Single scans recorded at low laser power reveal a similar width for strong lines with high J quantum numbers, where the fine structure splitting should be below 0.005 cm^{-1}. In any case, the observed width provides a lower limit for the lifetime of the ν_3 state levels of approximately 130 ps.

5.2. ν_1 Band. In contrast to the ν_3 band, the fine structure of the ν_1 transition could not be resolved owing to homogeneous line broadening induced by fast vibrational predissociation (Figure 5). From the observed line width of 0.2 cm^{-1}, the lifetime of the ν_1 excited state could be determined as ≈25 ps. The electron spin fine structure interaction terms were therefore neglected for the rotational analysis of this band. In addition, the rotational and centrifugal distortion constants of the ground vibrational state were fixed to the values determined from the analysis of the ν_3 band.

In total, 48 lines could be assigned within the ν_1 band, over J quantum numbers from 2 to 35. Upper state perturbations centered at $J = 15$, 18, and 33 produced deviations of 0.3, 0.2, and 0.1 cm^{-1} from the unperturbed energies, respectively. Therefore, the lines terminating in levels with $J = 12-23$ and $J = 33$ were not included in the analysis. The remaining weighted 33 lines could be fitted within 0.05 cm^{-1}, resulting in a standard deviation of 0.02 cm^{-1}. These values are in line with the observed line width of 0.2 cm^{-1}. The molecular constants derived from the final fit are listed in Table 2.

5.3. Other Vibrational Bands. The rotational structure of the other weak bands were only partly resolved, preventing the usual rotational analysis. However, as the positions of the respective band origins, band heads, and Q branches were prominent for these transitions, the following relationship was used to estimate the rotational constants of the upper and lower states:[62]

$$\nu_H - \nu_0 = -\frac{(B' + B'')^2}{4(B' - B'')} \qquad (2)$$

In the actual analysis, the effects of the centrifugal distortion in the upper and lower vibrational states were also included, wherein the D constants were constrained to either the ground or ν_1 state values depending on the degree of ν_1 excitation. The latter restriction will cause somewhat larger errors for transitions with heads at higher J levels. Table 3 summarizes the results obtained for the various transitions. They include the positions of the band centers and heads (with approximate J label) and the rotational constants obtained for lower and upper states. For comparison, the corresponding constants for the ground, ν_3, and ν_1 states derived from the detailed rotational analysis are presented as well. The rotational constant in the ν_s state determined from the $\nu_1 + \nu_s \leftarrow \nu_s$ transition was, within the uncertainties, the same as that derived from the analysis of the $\nu_1 \leftarrow \nu_s$ band, confirming the assignment of a common lower vibrational state.

6. Discussion

As the intermolecular interaction of the inert Ar atom with the NH_2^+ cation in its electronic ground state is weak, the electronic wave function of NH_2^+ is only slightly perturbed by complexation. The fine structure resolved in the ν_3 band clearly confirms that the triplet character of the ground state of the monomer is conserved in the complex. The ab initio calculations predict for both NH_2^+ and $Ar-NH_2^+$ a bent equilibrium geometry, however, with the barrier to linearity lying below the zero-point energy. The spectra of $Ar-NH_2^+$ provided no evidence for a semirigid nonlinear geometry, confirming the quasi-linearity of the complex.

The molecular constants extracted from the experimental spectra provide useful information about several properties of the intermolecular bond in each detected vibrational state (Table 4). Treating $Ar-NH_2^+$ as a pseudodiatomic molecule,[63] the intermolecular center of mass separation, R_{cm}, can be estimated from the rotational constants of the complex and the monomer under the assumption that the monomer geometry (r_{N-H} = 1.0251 Å) is not affected upon complexation. For the vibrational ground state of $Ar-NH_2^+$, a value of $R_{cm} = 3.0848(3)$ Å is obtained. This gives rise to a H−Ar separation of 2.0597(3) Å using a N−H separation of 1.025 10(4) Å, which was calculated from the rotational constant of the quasi-linear monomer (7.957 59(74) cm^{-1} [51]). According to the ab initio calculation, the bound N−H bond is lengthened by ca. 0.02 Å, which gives a corrected intermolecular Ar−H separation of 2.04 Å, in good agreement with the ab initio values of 2.02 and 1.99 Å for the bent and linear structures, respectively. The harmonic force constant (k_s) and frequency (ω_s) of the intermolecular stretching vibration derived from the molecular constants are 19.7(3) N/m and 171(1) cm^{-1}. The latter value is consistent with the ab initio frequency of around 185 cm^{-1} and the value extracted from hot and sequence bands, $\nu_s = 170.4(6)$ cm^{-1}.

Excitation of ν_1 leads to a considerable increase of the intermolecular interaction, as indicated by the increased values for k_s (28(5) N/m) and ω_s (203(17) cm^{-1}). The harmonic intermolecular stretching frequency compares well with the measured value of 197.2(8) cm^{-1}. The intermolecular separation in the ν_1 state is by approximately 0.05 Å shorter than that of the ground state. Excitation of ν_3 also leads to a stabilization of the intermolecular bond; however, the effects are much smaller compared to ν_1. The slight decrease in the intermolecular bond length (≤0.001 Å) is accompanied by a small increase in k_s (20.8(3) N/m) and ω_s (175.5(1.0) cm^{-1}). The approximate rotational constants of the ν_s and $\nu_s + \nu_1$ states in Table 3 indicate that the intermolecular bond stretches by 0.03(1)

TABLE 3: Vibrational Assignments of the Observed Transitions of $Ar-NH_2^+$[g]

transition	ν_0	ν_H	head	B'[a]	B''[a]
ν_3	3287.35699(81)[b]			0.152 040(25)	0.151 965(25)
ν_1	2803.647(11)[b]	2799.23(50)	P(28)	0.157 181(66)	0.151 965[c]
$\nu_1 + \nu_s$	3000.80(50)	2988.30(30)	P(67)	0.153 16(71)	0.151 965[c]
$\nu_1 + \nu_s \leftarrow \nu_s$	2830.30(80)	2825.70(20)	P(30)	0.153 16[d]	0.148 4(11)
$\nu_1 \leftarrow \nu_s$	2633.30(60)	2630.30(20)	P(19)	0.157 181[e]	0.149 4(16)
$\nu_1 \leftarrow \nu_b$[f]	2667.60(30)	2661.65(10)	P(37)	0.157 181[e]	0.153 34(28)

[a] Rotational constants obtained from analysis of the position of the band origins and band heads (except for ν_1 and ν_3). [b] Absolute accuracy of calibration is 0.01 cm^{-1}. [c] Fixed to value determined from the analysis of the ν_3 band. [d] Fixed to value determined from the analysis of the $\nu_1 + \nu_s$ band. [e] Fixed to value determined from the analysis of the ν_1 band. [f] Uncertain assignment. [g] Listed are band origins (ν_0), band heads (ν_H) with estimated J assignments, and rotational constants of the lower and upper states of the respective transitions. Figures in parentheses are estimated 1σ error limits. All values are given in cm^{-1}.

TABLE 4: Parameters of the Intermolecular Bond in Various Vibrational States of $Ar-NH_2^+$ Extracted from the Molecular Constants by Treating the Complex as a Pseudodiatomic Molecule[a]

parameter	ground state	ν_3	ν_1
R_{cm} (Å)	3.0848(3)	3.0840(3)	3.0321(6)
R_{H-Ar} (Å)	2.0597(3)	2.0589(3)	2.007(6)
k_s (N/m)	19.7(3)	20.8(3)	28(5)
ω_s (cm^{-1})	171(1)	175.5(1.0)	203(17)
ν_s (cm^{-1})	170.35(60)		197.2(8)

[a] Also given are the experimental values for ν_S.

Å upon excitation of ν_s in both the intramolecular ground and ν_1 excited states. In contrast, excitation of the intermolecular bending mode shortens the vibrationally averaged H−Ar separation by 0.012(5) Å. Such a contraction is typical for bending modes of linear rod and ball complexes and supports the assignment of the $\Sigma-\Pi$ type transition at 2668 cm^{-1} to the $\nu_1 \leftarrow \nu_b$ hot band.

The significant effects of ν_1 excitation on the molecular properties can be rationalized in the following way. As the ν_1 vibration corresponds mainly to the bound N−H stretch, vibrational excitation of this mode leads to significant stretching of this bond. The induced proton transfer toward the Ar ligand enhances the Ar−H interaction. This stabilization of the intermolecular bond causes the intramolecular N−H bond to become weaker, and both effects are visible in the respective frequency shifts: ν_1 decreases considerably upon complexation, while ν_s increases upon ν_1 excitation. On the other hand, excitation of the free N−H stretch (ν_3) has almost no effect on the properties of the intermolecular bond.

The ab initio calculations predict an intermolecular well depth $D_e = 1773$ cm^{-1} for the ground vibrational state. The observed complexation-induced frequency shifts are a measure of the changes in the intermolecular binding energy (D_0) upon excitation of the respective vibration. For the ν_3 vibration, which corresponds to the asymmetric stretch in the monomer and the free stretch in the dimer, the measured red shift of 72.6 cm^{-1} indicates that the interaction increases only slightly upon vibrational excitation, consistent with the conclusions drawn from the rotational analysis. The frequency of the symmetric stretch (ν_1) of the monomer is not known experimentally, and calculated values obtained from a simple valence-bond model of a linear symmetric XY_2 molecule (3143 cm^{-1} [64]), ab initio calculations (3088 and 3070 cm^{-1}, see Table 1), and rovibrational calculations (3128.4,[44] 3118,[42] 3051.43,[45] 3052.3,[43] and 3135.98 cm^{-1} [46]) range from 3050 to 3150 cm^{-1}. Thus, the ν_1 origin of the complex at 2803.6 cm^{-1} implies a complexation-induced red shift of the order of 300 ± 50 cm^{-1}. As ν_1 can be interpreted as bound N−H stretch in the complex, such a large shift is expected and compatible with the rotational analysis of the ν_1 band.

The observed predissociation lifetimes of 25 ps in the ν_1 state and ≥130 ps in the higher lying ν_3 state indicate that the involved dynamical processes are nonstatistical and highly mode-selective. The rapid energy transfer from the ν_1 state to the intermolecular degrees of freedom results from an efficient coupling of the bound N−H stretch and intermolecular stretch motions. On the other hand, this coupling is weak for the free N−H stretch leading to the substantially longer lifetime. A similar effect has been noted previously for other neutral[65] and ionic complexes.[66] A correlation between the predissociation rate and the square of the complexation-induced frequency shifts has been found experimentally for a variety of complexes,[67] and a theoretical model explaining this relation has been developed.[68] This rule appears to be compatible with the observations for the ν_1 and ν_3 modes of $Ar-NH_2^+$. It predicts the ν_3 lifetime to be of the order of 450 ± 150 ps, consistent with the lower limit of 130 ps derived from the experiment.

It is instructive to compare the properties of the quasi-linear $Ar-NH_2^+$ complex with those of the related closed-shell linear proton-bound Ar−HCO+ complex.[18,52] The interaction strength in proton-bound complexes of the type $B-HA^+$ is related to the difference in the proton affinities (PA) of the two bases A and B. As the PA of CO and NH are almost identical (600 vs 590 kJ/mol[35]) and much higher than that of Ar (371 kJ/mol[69]), the intermolecular bonds of their protonated ions with Ar should feature very similar properties. Indeed, the calculated binding energy of $Ar-HCO^+$ [70] is close to that of $Ar-NH_2^+$ ($D_e = 1551$ vs 1773 cm^{-1}) derived at the same level of theory. The slightly weaker bond in $Ar-HCO^+$ [18] is reflected in a smaller harmonic force constant for the intermolecular stretch vibration (17.0 vs 19.7(3) N/m) and a larger Ar−H separation (2.158 vs 2.06 Å). Moreover, the red shift in the ν_1 vibration (274 vs 300 ± 50 cm^{-1}) also appears to be slightly smaller in $Ar-HCO^+$.[52]

In contrast to the rotational and centrifugal distortion constants, which provide information mainly on the structure and intermolecular bond strength of the $Ar-NH_2^+$ complex, the parameter describing the electron spin interaction in the open-shell diradical complex contains information on the angular part of the intermolecular potential energy surface.[30,33,34] Assuming that the electromagnetic properties of NH_2^+ are not affected by the weak interaction with the Ar ligand, the spin−spin constant of the complex depends on the spin−spin constant of the monomer and the degree of zero-point bending excursion of the monomer within the complex[34]

$$\lambda_{Ar-NH_2^+} = \lambda_{NH_2^+} \langle {}^1/_2(3\cos^2\theta - 1)\rangle \qquad (3)$$

Using a monomer value of $\lambda_{NH_2^+} = 1.035(13)$ cm^{-1},[51] one obtains $\langle\cos^2\theta\rangle = 0.916(4)$ and $\langle\theta^2\rangle^{1/2} = 16.6(4)°$ for the ground state of the complex. This intermolecular bending angle corresponds to a harmonic frequency for the intermolecular

bending vibration of 190(9) cm^{-1}. In section 4 the band at 2667.6 cm^{-1} has tentatively been assigned to the $\nu_1 \leftarrow \nu_b$ hot band, which would result in a somewhat lower bending frequency of 136 cm^{-1}. The discrepancy between these two values may arise from the deficiencies of the model, which neglects the effects of anharmonicity, angular-radial coupling, and quasi-linearity, or from a misassignment of the 2667.6 cm^{-1} transition.

One or more overlapping weak transitions with unidentified symmetry are observed in the 3465−3485 cm^{-1} region. A sharp feature centered at 3475.7(3) cm^{-1} could either be a Q branch of a $\Pi-\Sigma$ transition or a highly degraded P or R branch band head of a $\Sigma-\Sigma$ transition. Weak signals appear to both sides of the sharp feature. One possible candidate for a $\Sigma-\Sigma$ type transition is the $\nu_3 + \nu_s$ band. The ν_s frequency in the intramolecular ground state was deduced as 170.4 cm^{-1}. From the rotational analysis of the ν_3 band one can estimate that the ν_s frequency increases by around 5 cm^{-1} upon ν_3 excitation, giving rise to a predicted band origin of 3463 cm^{-1} for $\nu_3 + \nu_s$. Thus, part of the weak structure to the red of the sharp feature may be due to $\nu_3 + \nu_s$. Contour simulations using reasonable upper state rotational constants (estimated from the ν_s state) show, however, that the sharp feature is probably not due to a R branch head of $\nu_3 + \nu_s$. Therefore, an assignment of this feature to the Q branch of $\nu_3 + \nu_b$ has been considered. This would give rise to a bending frequency of 188 cm^{-1}, which would be compatible with the harmonic value deduced from the spin−spin constant (see above). However, it is significantly higher than the value deduced from the $\nu_1 \leftarrow \nu_b$ hot band, $\nu_b = 136$ cm^{-1}, questioning either of the two assignments, as the intermolecular bond is almost not affected upon ν_3 excitation. An alternative assignment to the intramolecular combination band $\nu_1 + \nu_2$ leads to a frequency for ν_2 of ~ 672 cm^{-1}. This value is much higher than the estimated monomer fundamental frequency of $\nu_2^{linear} = 336$ cm^{-1}.[46] Though intramolecular bending frequencies of linear molecules usually increase substantially upon formation of linear complexes with rare gas atoms, the complications arising from the quasi-linearity prevent a reliable estimate of this effect in $Ar-NH_2^+$. Thus, the definitive assignment of the structure observed in the 3465−3485 cm^{-1} range awaits further experimental and/or theoretical data.

7. Conclusion

The electronic ground state of the $Ar-NH_2^+$ radical ionic complex has been studied by both high-resolution IR predissociation spectroscopy and ab initio calculations at the UMP2 level of theory. The results, which represent the first spectroscopic and theoretical characterization for this diradical cluster, can be summarized as follows.

The complex has a quasi-linear proton-bound $Ar-HNH^+$ structure in its $^3\Sigma^-$ ground state, and the intermolecular bond is characterized by a binding energy $D_e = 1773$ cm^{-1}, an intermolecular Ar−H separation of approximately 2.04 Å, and a harmonic intermolecular stretching force constant of 19.7(3) N/m. Both the calculations and the rotational structure of the observed transitions show that complexation with Ar has only a small effect on the quasi-linearity of HNH^+ and does not change its diradical character. In contrast, complexation has a drastic effect on the properties of the N−H stretch normal coordinates. The asymmetric (ν_3) and symmetric (ν_1) N−H stretch vibrations of the monomer are transformed into a free and bound N−H stretch in the complex, respectively. While the intermolecular interaction in the ν_3 state is similar to that in the vibrational ground state, excitation of the ν_1 vibration leads to a significantly stronger, and thus shorter, intermolecular bond. The latter effect can be explained by a partial transfer of the intermediate proton from N to Ar, which results in the destabilization of the bound N−H bond. The free N−H bond is nearly unaffected. In addition, the observed predissociation lifetimes were found to be mode-selective. The much shorter lifetime of the ν_1 state (25 ps) compared to the higher-lying ν_3 state ($\geq$130 ps) arises from the more efficient coupling of the bound N−H stretch vibration to the intermolecular stretching mode as compared to the free N−H stretch. The complexation-induced 12.5% decrease of the spin−spin interaction constant results from the large amplitude intermolecular bending vibration and corresponds in the rod and ball model to an average intermolecular bending angle of 17°. In general, the properties of the intermolecular bond in the $Ar-HNH^+$ complex were found to be close to those of the previously studied $Ar-HCO^+$ complex, and this observation has been rationalized by the similar proton affinities of NH and CO.

Acknowledgment. This study is part of the Project No. 20-49104.96 of the Swiss National Science Foundation.

References and Notes

(1) Hobza, P.; Zahradnik, R. *Intermolecular Complexes: The Role of van der Waals Systems in Physical Chemistry and in the Biodisciplines*; Elsevier: Amsterdam, 1988.
(2) Hirschfelder, J. O.; Curtis, C. F.; Bird, R. B. *Molecular Theory of Gases and Liquids*; Wiley: New York, 1954.
(3) Nesbitt, D. J. *Annu. Rev. Phys. Chem.* **1994**, *45*, 367.
(4) Leopold, K. R.; Fraser, G. T.; Novick, S. E.; Klemperer, W. *Chem. Rev.* **1994**, *94*, 1807.
(5) Bacic, Z.; Miller, R. E. *J. Phys. Chem.* **1996**, *100*, 12945.
(6) Cohen, R. C.; Saykally, R. J. *J. Phys. Chem.* **1992**, *96*, 1024.
(7) Legon, A. C.; Millen, D. J. *Chem. Rev.* **1986**, *86*, 635.
(8) Hutson, J. M. *Annu. Rev. Phys. Chem.* **1990**, *41*, 123.
(9) Hutson, J. M. *J. Chem. Phys.* **1992**, *96*, 6752.
(10) van der Avoird, A.; Wormer, P. E. S.; Moszynski, R. *Chem. Rev.* **1994**, *94*, 1931.
(11) Elrod, M. J.; Saykally, R. J. *Chem. Rev.* **1994**, *94*, 1975.
(12) Bieske, E. J.; Maier, J. P. *Chem. Rev.* **1993**, *93*, 2603.
(13) Müller-Dethlefs, K.; Dopfer, O.; Wright, T. G. *Chem. Rev.* **1994**, *94*, 1845.
(14) Duncan, M. A. *Annu. Rev. Phys. Chem.* **1997**, *48*, 69.
(15) Lisy, J. M. In *Cluster Ions*; Ng, C.-Y., Baer, T., Powis, I., Eds.; Wiley: New York, 1993; p 217.
(16) Carrington, A.; Shaw, A. M.; Taylor, S. M. *J. Chem. Soc., Faraday. Trans.* **1995**, *91*, 3725.
(17) Bogey, M.; Bolvin, H.; Demuynck, C.; Destombes, J. L. *Phys. Rev. Lett.* **1987**, *58*, 988.
(18) Oshima, Y.; Sumiyoshi, Y.; Endo, Y. *J. Chem. Phys.* **1997**, *106*, 2977.
(19) Speck, T.; Linnartz, H.; Maier, J. P. *J. Chem. Phys.* **1997**, *107*, 8706.
(20) Linnartz, H.; Speck, T.; Maier, J. P. *Chem. Phys. Lett.* **1998**, *288*, 504.
(21) Okumura, M.; Yeh, L. I.; Lee, Y. T. *J. Chem. Phys.* **1985**, *83*, 3705.
(22) Meot-Ner, M. *J. Am. Chem. Soc.* **1984**, *106*, 1257.
(23) Nizkorodov, S. A.; Maier, J. P.; Bieske, E. J. *J. Chem. Phys.* **1995**, *103*, 1297.
(24) Olkhov, R. V.; Nizkorodov, S. A.; Dopfer, O. *J. Chem. Phys.* **1997**, *107*, 8229.
(25) Nizkorodov, S. A.; Spinelli, Y.; Bieske, E. J.; Maier, J. P.; Dopfer, O. *Chem. Phys. Lett.* **1997**, *265*, 303.
(26) Nizkorodov, S. A.; Maier, J. P.; Bieske, E. J. *J. Chem. Phys.* **1995**, *102*, 5570.
(27) Olkhov, R. V.; Nizkorodov, S. A.; Dopfer, O. *Chem. Phys.*, in press.
(28) Dopfer, O.; Nizkorodov, S. A.; Meuwly, M.; Bieske, E. J.; Maier, J. P. *Int. J. Mass Spectrom. Ion Processes* **1997**, *167−168*, 637.
(29) Nizkorodov, S. A.; Roth, D.; Olkhov, R. V.; Maier, J. P.; Dopfer, O. *Chem. Phys. Lett.* **1997**, *278*, 26.
(30) Roth, D.; Nizkorodov, S. A.; Maier, J. P.; Dopfer, O. *J. Chem. Phys.* **1998**, *109*, 3841.
(31) Nizkorodov, S. A.; Dopfer, O.; Meuwly, M.; Maier, J. P.; Bieske, E. J. *J. Chem. Phys.* **1996**, *105*, 1770.
(32) Fawzy, W. M. *J. Mol. Spectrosc.* **1993**, *160*, 84.

(33) Qian, H.-B.; Low, S. J.; Seccombe, D.; Howard, B. J. *J. Chem. Phys.* **1997**, *107*, 7651.
(34) Qian, H.-B.; Seccombe, D.; Howard, B. J. *J. Chem. Phys.* **1997**, *107*, 7658.
(35) Huntress, W. T. *Astrophys. J. Suppl.* **1977**, *33*, 495.
(36) Herbst, E.; Klemperer, W. *Astrophys. J.* **1973**, *185*, 505.
(37) Dalgarno, A. In *Interactions between Ions and Molecules*; Ausloos, P., Ed.; Plenum Press: New York, 1975; p 341.
(38) Gerlich, D. *J. Chem. Soc., Faraday Trans.* **1993**, *89*, 2199.
(39) Lee, S. T.; Morokuma, K. *J. Am. Chem. Soc.* **1971**, *93*, 6863.
(40) Peyerimhoff, S. D.; Buenker, R. *J. Chem. Phys.* **1979**, *42*, 167.
(41) DeFrees, D. J.; McLean, A. D. *J. Chem. Phys.* **1985**, *82*, 333.
(42) Jensen, P.; Bunker, P. R.; McLean, A. D. *Chem. Phys. Lett.* **1987**, *141*, 53.
(43) Barcley, V. J.; Hamilton, I. P.; Jensen, P. *J. Chem. Phys.* **1993**, *99*, 9709.
(44) Chambaud, G.; Gabriel, W.; Schmelz, T.; Rosmus, P.; Spielfiedel, A.; Feautrier, N. *Theor. Chim. Acta* **1993**, *87*, 5.
(45) Jensen, P. *J. Mol. Spectrosc.* **1997**, *181*, 207.
(46) Osman, G.; Bunker, P. R.; Jensen, P.; Kraemer, W. P. *J. Mol. Spectrosc.* **1997**, *186*, 319.
(47) Stephens, J. C.; Yamaguchi, Y.; Sherrill, C. D.; Schaefer, H. F., III *J. Phys. Chem. A* **1998**, *102*, 3999.
(48) Dunlavey, S. J.; Dyke, J. M.; Jonathan, N.; Morris, A. *Mol. Phys.* **1980**, *39*, 1121.
(49) Gibson, S. T.; Greene, J. P.; Berkowitz, J. *J. Chem. Phys.* **1985**, *83*, 4319.
(50) Okumura, M.; Rehfus, B. D.; Dinelli, B. M.; Bawendi, M. G.; Oka, T. *J. Chem. Phys.* **1989**, *90*, 5918.
(51) Kabbadj, Y.; Huet, T. R.; Uy, D.; Oka, T. *J. Mol. Spectrosc.* **1996**, *175*, 277.
(52) Nizkorodov, S. A.; Dopfer, O.; Ruchti, T.; Meuwly, M.; Maier, J. P.; Bieske, E. J. *J. Phys. Chem.* **1995**, *99*, 17118.
(53) Bieske, E. J. *J. Chem. Soc., Faraday Trans.* **1995**, *91*, 1.
(54) Daly, N. R. *Rev. Sci. Instrum.* **1960**, *31*, 264.
(55) Guelachvili, G.; Rao, K. N. *Handbook of Infrared Standards*; Academic Press: London, 1993; Vols. 1 and 2.
(56) Frisch, M. J.; Trucks, G. W.; Schlegel, H. B.; Gill, P. M. W.; Johnson, B. G.; Robb, M. A.; Cheeseman, J. R.; Keith, T.; Petersson, G. A.; Montgomery, J. A.; Raghavachari, K.; Al-Laham, M. A.; Zakrzewski, V. G.; Ortiz, J. V.; Foresman, J. B.; Cioslowski, J.; Stefanov, B. B.; Nanayakkara, A.; Challacombe, M.; Peng, C. Y.; Ayala, P. Y.; Chen, W.; Wong, M. W.; Andres, J. L.; Replogle, E. S.; Gomperts, R.; Martin, R. L.; Fox, D. J.; Binkley, J. S.; Defrees, D. J.; Baker, J.; Stewart, J. P.; Head-Gordon, M.; Gonzales, C.; Pople, J. A. *GAUSSIAN 94;* Gaussian, Inc: Pittsburgh, PA, 1995.
(57) Extensible Computational Chemistry Environmental Basis Set Data Base, Version 10, 1996.
(58) Boys, S. F.; Bernardi, F. *Mol. Phys.* **1970**, *19*, 553.
(59) Chalasinski, G.; Szczesniak, M. M. *Chem. Rev.* **1994**, *94*, 1.
(60) Nizkorodov, S. A.; Meuwly, M.; Maier, J. P.; Dopfer, O.; Bieske, E. J. *J. Chem. Phys.* **1998**, *108*, 8964.
(61) Meuwly, M.; Nizkorodov, S. A.; Maier, J. P.; Bieske, E. J. *J. Chem. Phys.* **1996**, *104*, 3876.
(62) Herzberg, G. *Molecular Spectra and Molecular Structure*; Van Nostrand: New York, 1950; Vol 1.
(63) Millen, D. C. *Can. J. Chem.* **1985**, *63*, 1477.
(64) Herzberg, G. *Molecular Spectra and Molecular Structure*; Krieger: Malabar, 1991; Vol 2.
(65) Miller, R. E. *Acc. Chem. Res.* **1990**, *23*, 10.
(66) Bieske, E. J.; Nizkorodov, S. A.; Bennett, F. R.; Maier, J. P. *J. Chem. Phys.* **1995**, *102*, 5152.
(67) Miller, R. E. *Science* **1988**, *240*, 447.
(68) LeRoy, R. J.; Davies, M. R.; Lam, M. E. *J. Phys. Chem.* **1991**, *95*, 2167.
(69) Lias, S. G.; Bartmess, J. E.; Liebman, J. F.; Holmes, J. L.; Levin, R. D.; Mallard, W. G. *J. Phys. Chem. Ref. Data* **1988**, 17.
(70) Dopfer, O. Unpublished results.